

# Supporting Information

## Simple structure descriptors quantifying the diffusion of ethene in small-pore zeolites: Insights from molecular dynamic simulations

Guang Yang,<sup>a</sup> Chuan-Ming Wang,<sup>\*a</sup> Yi Li,<sup>b</sup> Yu-Jue Du,<sup>a</sup> Yang-Dong Wang,<sup>a</sup> Zai-Ku Xie<sup>\*a</sup>

*<sup>a</sup>State Key Laboratory of Green Chemical Engineering and Industrial Catalysis, Sinopec Shanghai Research Institute of Petrochemical Technology, Shanghai 201208, China*

*<sup>b</sup>State Key Laboratory of Inorganic Synthesis and Preparative Chemistry, College of Chemistry, Jilin University, Changchun 130012, China*

## S1. Force field

The PCFF force field in LAMMPS package was used in class II force field type<sup>[1]</sup> for bond, angle, dihedral, improper, and cross terms. To model the intra- and inter-molecular interactions between zeolite and guest molecules, various potential types as listed in Table S1 were employed to calculate total energies using the following formula,

$$E_{total} = E_{bonds} + E_{angles} + E_{bond-bond} + E_{angle-angle} + E_{improper} + E_{bond-angle} + E_{dihedral} + E_{middle-bond-torsion} + E_{end-bond-torsion} + E_{angle-torsion} + E_{angle-angle-torsion} + E_{LJ} + E_{coulomb} \quad (1)$$

For the zeolite,  $E_{improper}$ ,  $E_{middle-bond-torsion}$ ,  $E_{end-bond-torsion}$  and  $E_{angle-torsion}$  were not considered. The Lennard-Jones (LJ) 9-6 function ( $E_{LJ}$ ) was used to model the van der Waals interactions,

$$E_{LJ}^{ij,9-6} = \varepsilon_{ij} \left\{ 2 \left[ \frac{\sigma_{ij}}{r} \right]^9 - 3 \left[ \frac{\sigma_{ij}}{r} \right]^6 \right\} \quad (2)$$

where  $\varepsilon_{ij}$  is the LJ well-depth potential,  $\sigma_{ij}$  is the effective LJ interaction diameter between atom  $i$  and  $j$ ,  $r$  is the actual distance of atom pair.

$$\varepsilon_{ij} = \frac{2\sqrt{\varepsilon_i \varepsilon_j} \sigma_i^3 \sigma_j^3}{\sigma_i^6 + \sigma_j^6} \quad (3)$$

$$\sigma_{ij} = \left( \frac{1}{2} (\sigma_i^6 + \sigma_j^6) \right)^{\frac{1}{6}} \quad (4)$$

where  $\sigma_i$ ,  $\sigma_j$ ,  $\varepsilon_i$  and  $\varepsilon_j$  represent the atom interaction parameters for atom  $i$  and  $j$ , respectively. The electrostatic potential is expressed by,

$$E_{coul} = \sum_{ij} \frac{Cq_i q_j}{\varepsilon r} \quad (5)$$

where  $C$  is an energy-conversion constant,  $q_i$  and  $q_j$  are the charges on two atoms, and  $\varepsilon$  is the dielectric constant. Tables S2 and S3 list the corresponding intra-molecular and inter-molecular potential parameters.

**Table S1.** Term details of Force field used to model zeolite framework and guest molecules.

$$E_{bond}(r) = K_2(r - r_0)^2 + K_3(r - r_0)^3 + K_4(r - r_0)^4 \quad (6)$$

$$E_{angle}(\theta) = K_2(\theta - \theta_0)^2 + K_3(\theta - \theta_0)^3 + K_4(\theta - \theta_0)^4 \quad (7)$$

$$E_{bond-bond}(r_{ij}, r_{jk}) = M(r_{ij} - r_1)(r_{jk} - r_2) \quad (8)$$

$$E_{bond-angle}(r_{ij}, \theta, r_{jk}) = N_1(r_{ij} - r_1)(\theta - \theta_0) + N_2(r_{jk} - r_2)(\theta - \theta_0) \quad (9)$$

$$E_{angle-angle}(\theta_{ijk}, \theta_{kjl}, \theta_{ijl}) = M_1(\theta_{ijk} - \theta_1)(\theta_{kjl} - \theta_3) + M_2(\theta_{ijk} - \theta_1)(\theta_{ijl} - \theta_2) + M_3(\theta_{ijl} - \theta_2)(\theta_{kjl} - \theta_3) \quad (10)$$

$$E_{improper}(x_{ijkl}, x_{kjli}, x_{ljik}) = K \left[ (x_{ijkl} + x_{kjli} + x_{ljik}) / 3 - x_0 \right]^2 \quad (11)$$

$$E_{dihedral}(\phi) = \sum_{n=1}^3 K_n [1 - \cos(n\phi - \phi_n)] \quad (12)$$

$$E_{middle-bond-torsion}(r_{jk}, \phi) = (r_{jk} - r_2)(A_1 \cos \phi + A_2 \cos 2\phi + A_3 \cos 3\phi) \quad (13)$$

$$E_{end-bond-torsion}(r_{ij}, \phi, r_{kl}) = (r_{ij} - r_1)(B_1 \cos \phi + B_2 \cos 2\phi + B_3 \cos 3\phi) + (r_{kl} - r_3)(C_1 \cos \phi + C_2 \cos 2\phi + C_3 \cos 3\phi) \quad (14)$$

$$E_{angle-torsion}(\theta_{ijk}, \phi, \theta_{jkl}) = (\theta_{ijk} - \theta_1)(D_1 \cos \phi + D_2 \cos 2\phi + D_3 \cos 3\phi) + (\theta_{jkl} - \theta_2)(E_1 \cos \phi + E_2 \cos 2\phi + E_3 \cos 3\phi) \quad (15)$$

$$E_{angle-angle-torsion}(\theta_{ijk}, \phi, \theta_{jkl}) = M(\theta_{ijk} - \theta_1)(\theta_{jkl} - \theta_2) \cos \phi \quad (16)$$

**Table S2.** Bonded potential parameters for zeolite framework and guest molecules.

$E_{bond}$	$K_2$	$K_3$	$K_4$	$r_0$ (Å <sup>2</sup> )
	(kcal/mol/Å <sup>2</sup> )	(kcal/mol/Å <sup>3</sup> )	(kcal/mol/Å <sup>4</sup> )	
Si-O	325.4430	-943.3640	1454.6700	1.6155
C-C	545.2663	-1005.6330	1225.7415	1.3521
C-H	365.7679	-725.5404	781.6621	1.0883
$E_{angle}$	$K_2$	$K_3$	$K_4$	$\theta_0$ (deg)
	(kcal/mol/rad <sup>2</sup> )	(kcal/mol/rad <sup>3</sup> )	(kcal/mol/rad <sup>4</sup> )	
Si-O-Si	18.8146	37.9749	42.8222	176.2650
O-Si-O	154.1860	-68.6595	23.6292	110.6120
C-C-H	35.2766	-17.7740	-1.6215	124.8800
H-C-H	29.6363	-12.4853	-6.2218	115.4900
$E_{bond-bond}$	$M$ (kcal/mol/Å <sup>2</sup> )	$r_1$ (Å)	$r_2$ (Å)	
Si-O~Si-O	178.8840	1.6155	1.6155	
C-C-H	10.1047	1.3521	1.0883	
H-C-H	4.8506	1.0883	1.0883	
$E_{bond-angle}$	$N_1$	$N_2$	$r_1$ (Å)	$r_2$ (Å)
	(kcal/mol/Å/rad)	(kcal/mol/Å/rad)		
Si-O-Si	13.4905	13.4905	1.6155	1.6155
O-Si-O	87.3528	87.3528	1.6155	1.6155
C-C-H	23.3588	19.0592	1.3521	1.0883
H-C-H	17.9795	17.9795	1.0883	1.0883
The $\theta_0$ value in the $E_{bond-angle}$ is the same value from the $E_{angle}$ formula.				
$E_{angle-angle}$	$M_1 = M_2 = M_3$ (kcal/mol/rad <sup>2</sup> )		$\theta_1 = \theta_2 = \theta_3$ (deg)	
O-Si-O~O-Si-O	9.0179		110.612	
$E_{improper}$	$K$ (kcal/mol/rad <sup>2</sup> )		$x_0$ (deg)	

C-C-H-H	2.8561		0	
$E_{dihedral}$	$K_1$ (kcal/mol)	$K_2$ (kcal/mol)	$K_3$ (kcal/mol)	$\phi_1 = \phi_2 = \phi_3$ (deg)
Si-O-Si-O	-0.3417	0.0961	0.1683	0
H-C-C-H	0	4.8974	0	0
$E_{middle-bond-torsion}$	$A_1$ (kcal/mol/Å)	$A_2$ (kcal/mol/Å)	$A_3$ (kcal/mol/Å)	$r_2$ (Å)
H-C-C-H	0.8558	6.3911	0	1.3521
$E_{end-bond-torsion}$	$B_1 = C_1$ (kcal/mol/Å)	$B_2 = C_2$ (kcal/mol/Å)	$B_3 = C_3$ (kcal/mol/Å)	$r_1 = r_3$ (Å)
H-C-C-H	0.7129	0.5161	0	1.0883
$E_{angle-torsion}$	$D_1 = E_1$ (kcal/mol/rad)	$D_2 = E_2$ (kcal/mol/rad)	$D_3 = E_3$ (kcal/mol/rad)	$\theta_1 = \theta_2$ (deg)
H-C-C-H	-1.8911	3.2540	0	124.880
$E_{angle-angle-torsion}$	$M$ (kcal/mol/rad <sup>2</sup> )	$\theta_1$ (deg)	$\theta_2$ (deg)	
Si-O-Si-O	5.7889	176.2650	110.6120	
H-C-C-H	-7.0058	124.880	124.880	

**Table S3.** Non-bonded LJ potential parameters for zeolite framework and guest molecules.

Site	$E_{LJ}$	$\sigma_{ij}$ (Å)	$\epsilon_{ij}$ (kcal/mol)	Charge(e)
O-O	LJ 9-6	3.300	0.0800	-0.4450
Si-Si	LJ 9-6	4.290	0.1050	0.8900
C-C	LJ 9-6	3.920	0.0800	-0.2536
H-H	LJ 9-6	2.878	0.0230	0.1268

### Reference

1. Ewig, C. S.; Thacher, T. S.; Hagler, A. T., Derivation of Class II Force Fields. 7. Nonbonded Force Field Parameters for Organic Compounds. *J Phys Chem B* **1999**, *103*, 6998-7014.

## S2. Figures

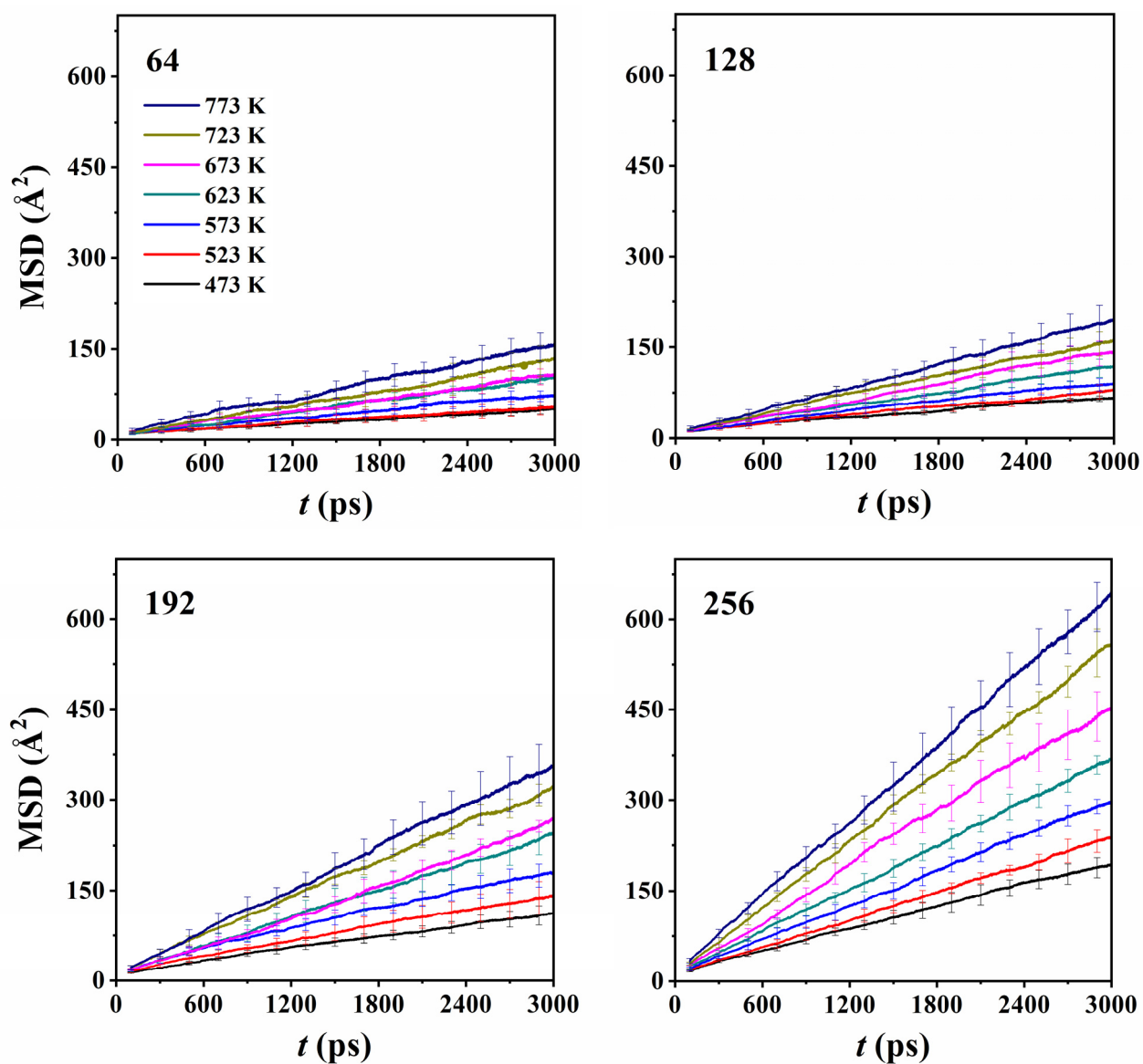


**Fig. S1** MSD (in the unit of  $\text{\AA}^2$ ) plots with error bars of ethene diffusion in LEV zeolite at seven temperatures. The molecular loading is 64, 128, 192, 256, respectively.

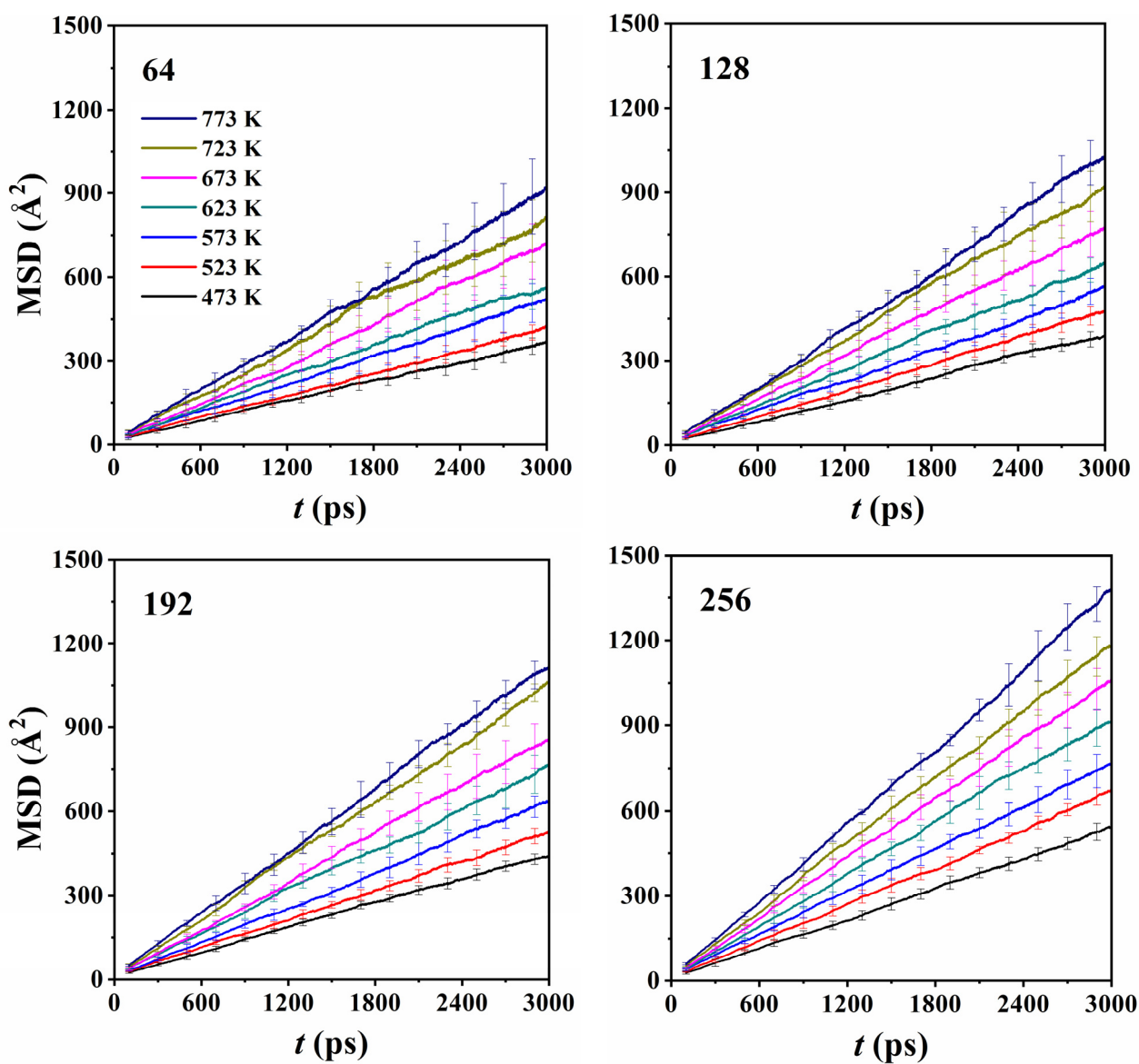


**Fig. S2** MSD (in the unit of  $\text{\AA}^2$ ) plots with error bars of ethene diffusion in CHA zeolite at seven temperatures. The molecular loading is 64, 128, 192, 256, respectively.



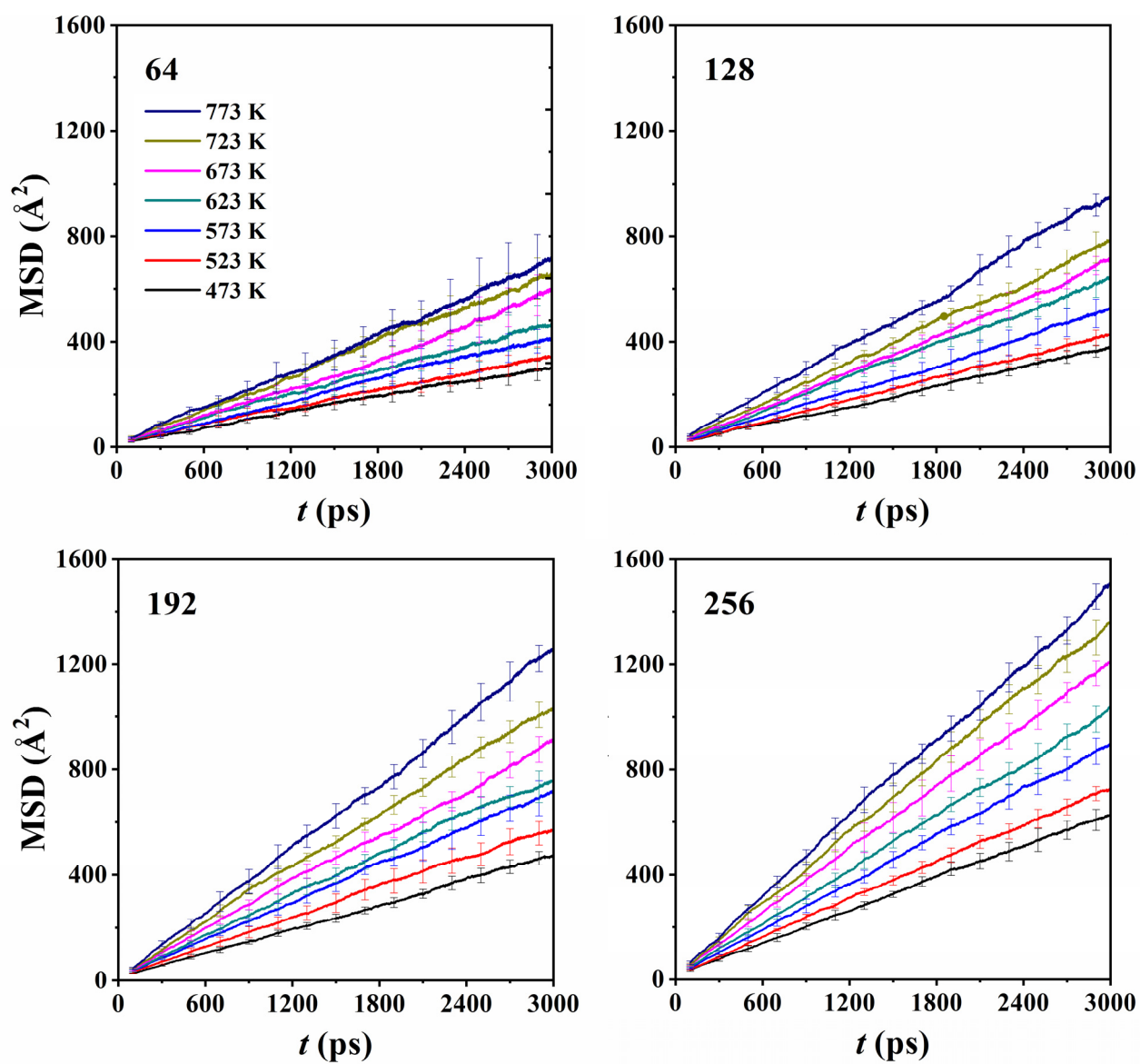


**Fig. S3** MSD (in the unit of  $\text{\AA}^2$ ) plots with error bars of ethene diffusion in AEI zeolite at seven temperatures. The molecular loading is 64, 128, 192, 256, respectively.

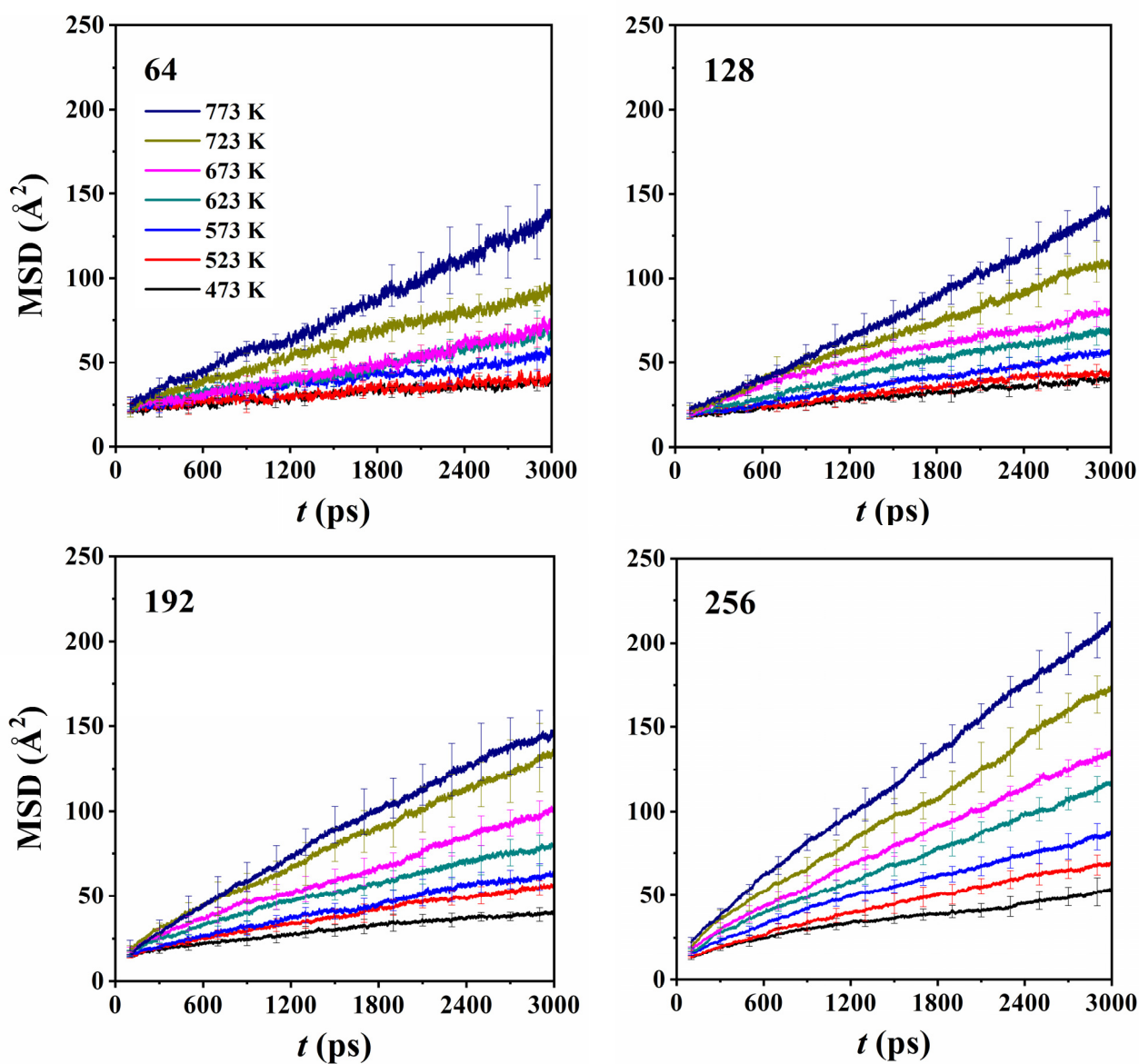


**Fig. S4** MSD (in the unit of  $\text{\AA}^2$ ) plots with error bars of ethene diffusion in ERI zeolite at seven temperatures. The molecular loading is 64, 128, 192, 256, respectively.

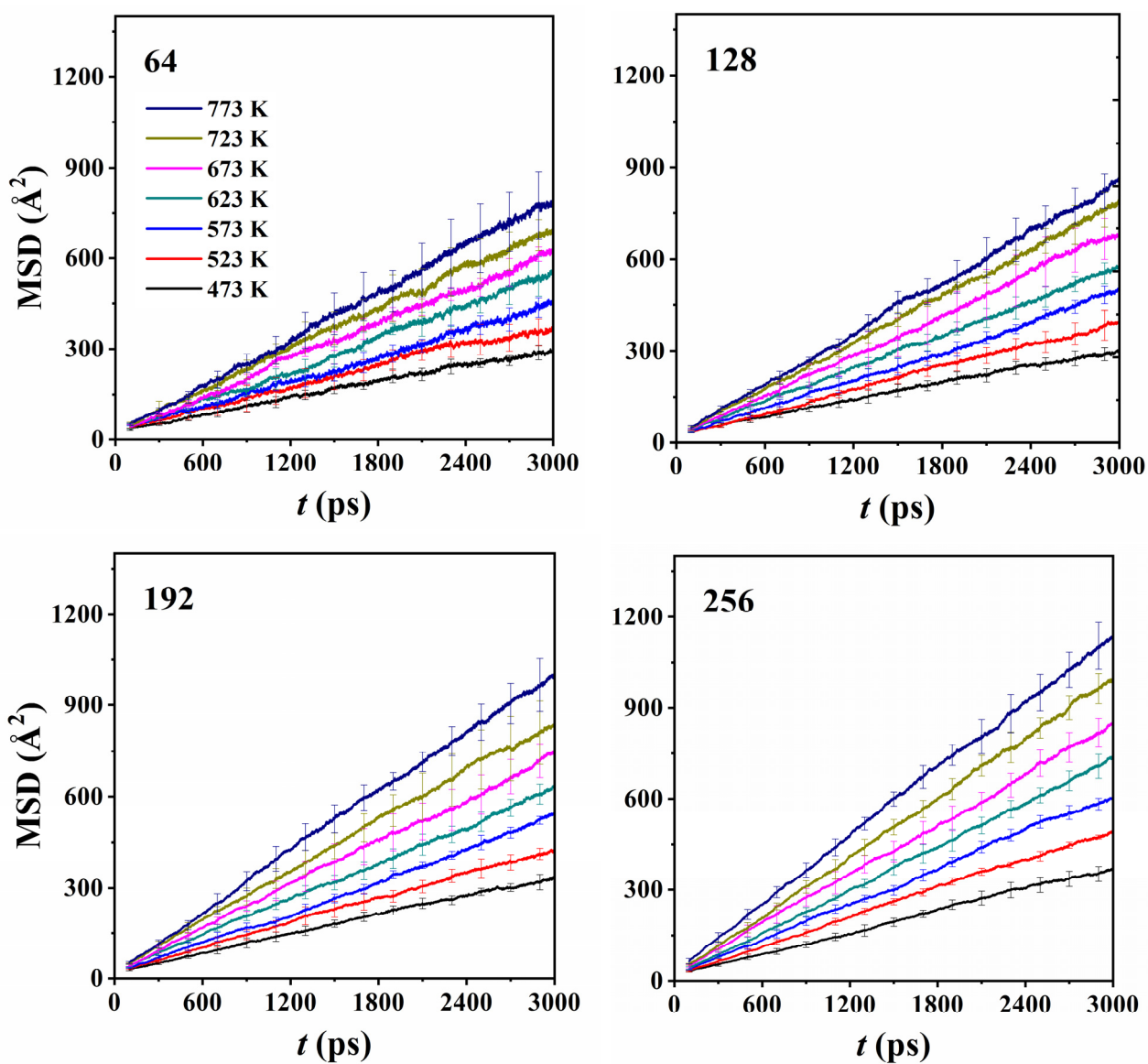


**Fig. S5** MSD (in the unit of  $\text{\AA}^2$ ) plots with error bars of ethene diffusion in AFX zeolite at seven temperatures. The molecular loading is 64, 128, 192, 256, respectively.

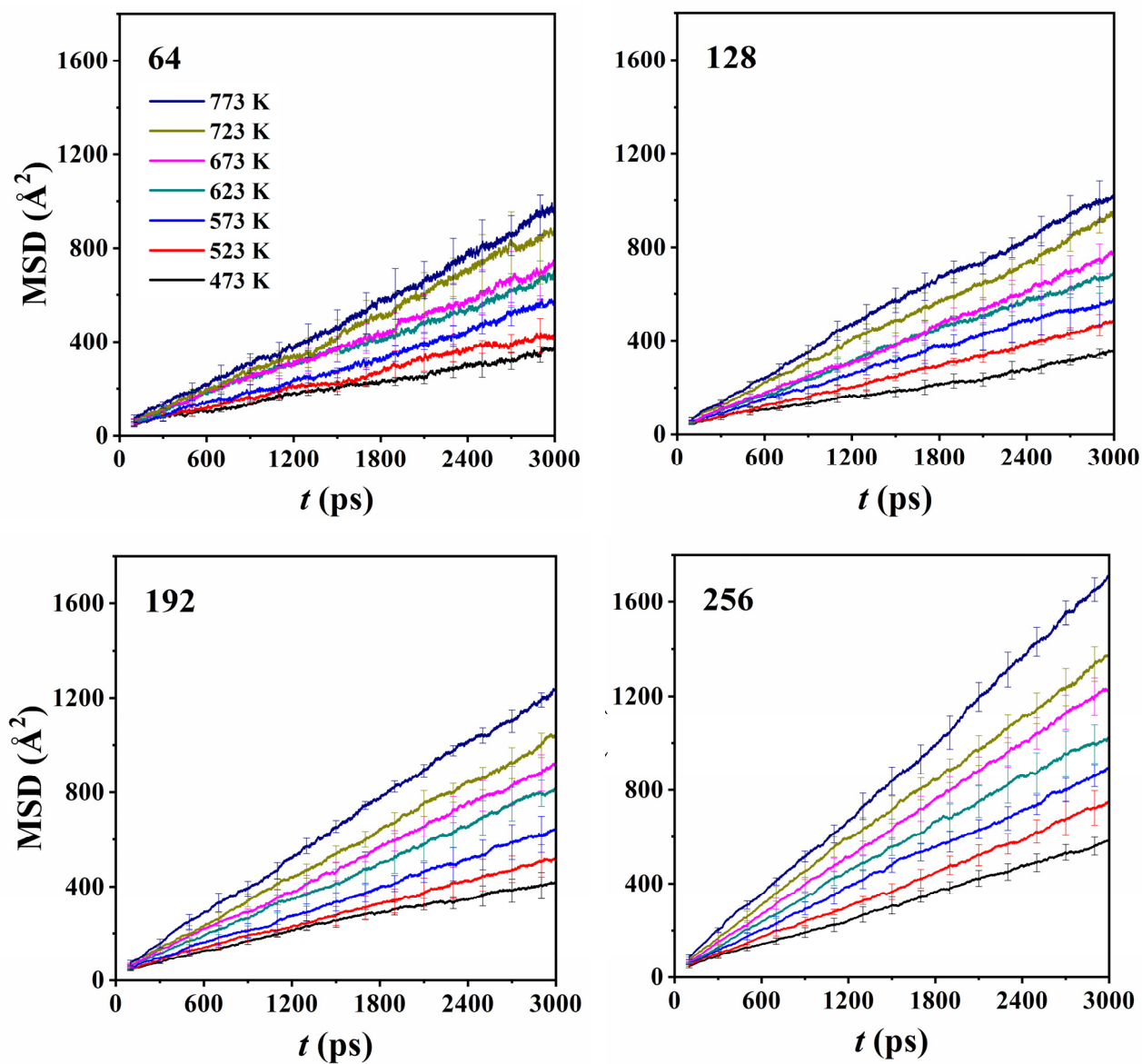


**Fig. S6** MSD (in the unit of  $\text{\AA}^2$ ) plots with error bars of ethene diffusion in SFW zeolite at seven temperatures. The molecular loading is 64, 128, 192, 256, respectively.

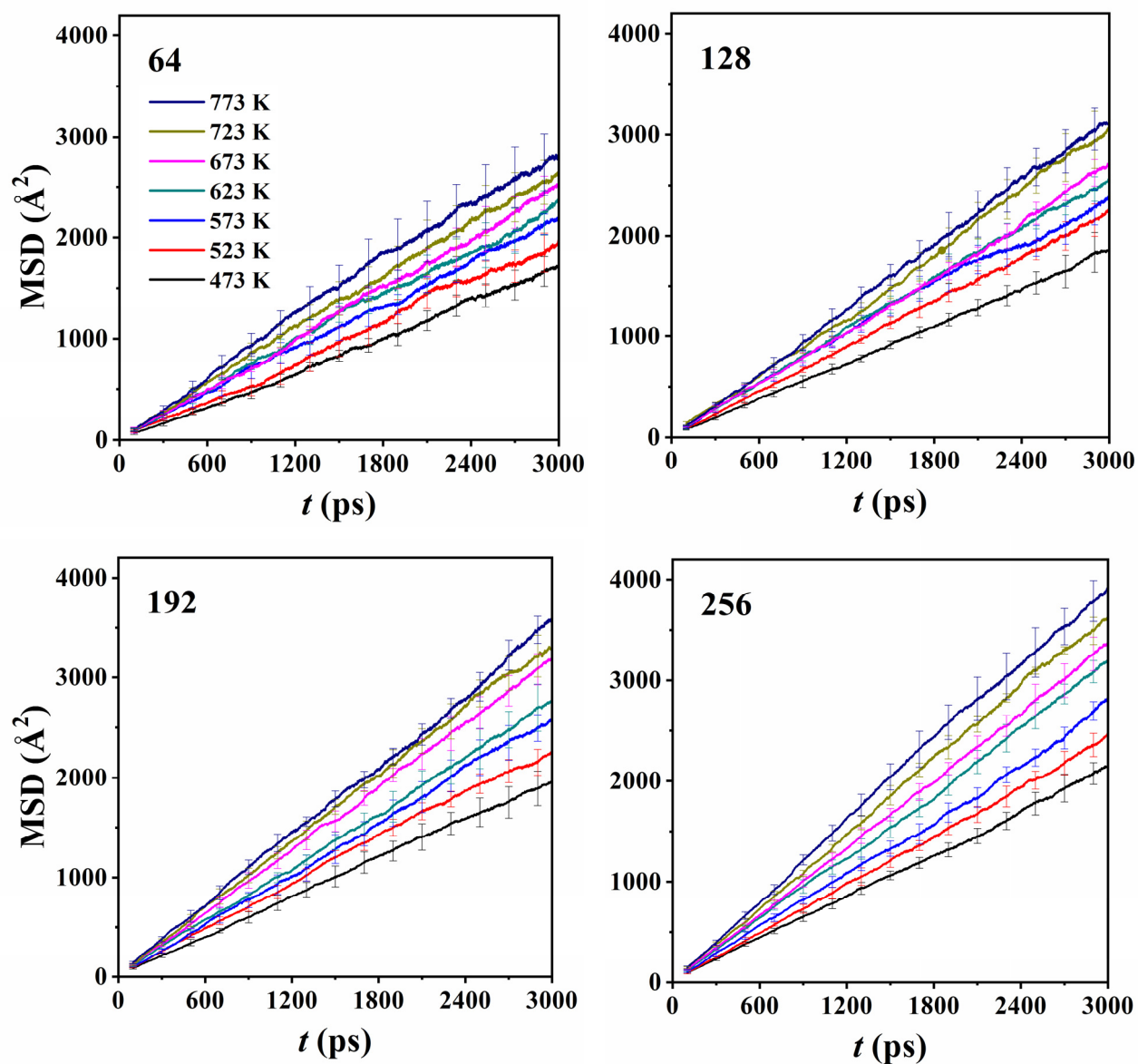


**Fig. S7** MSD (in the unit of  $\text{\AA}^2$ ) plots with error bars of ethene diffusion in RHO zeolite at seven temperatures. The molecular loading is 64, 128, 192, 256, respectively.

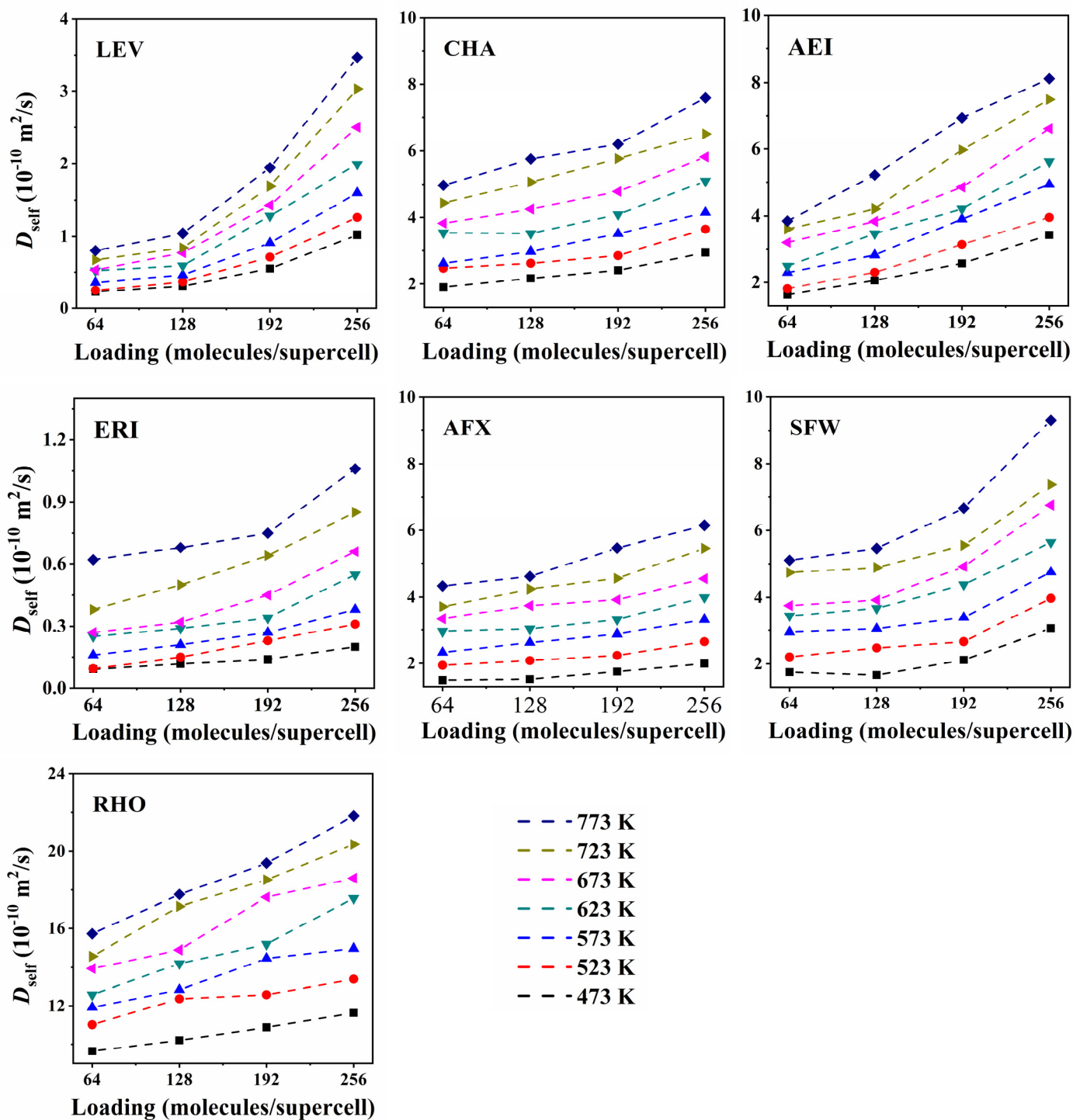
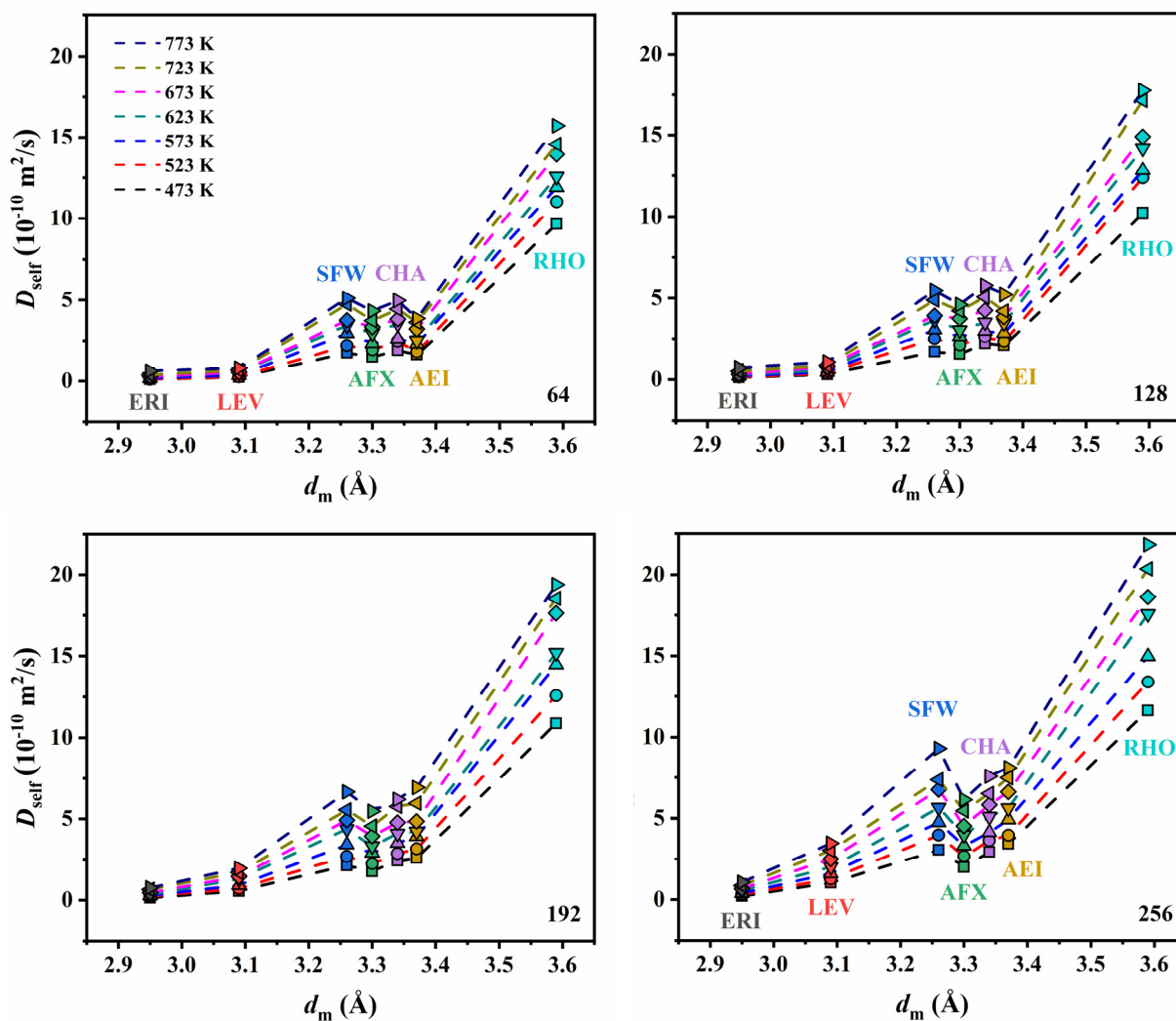
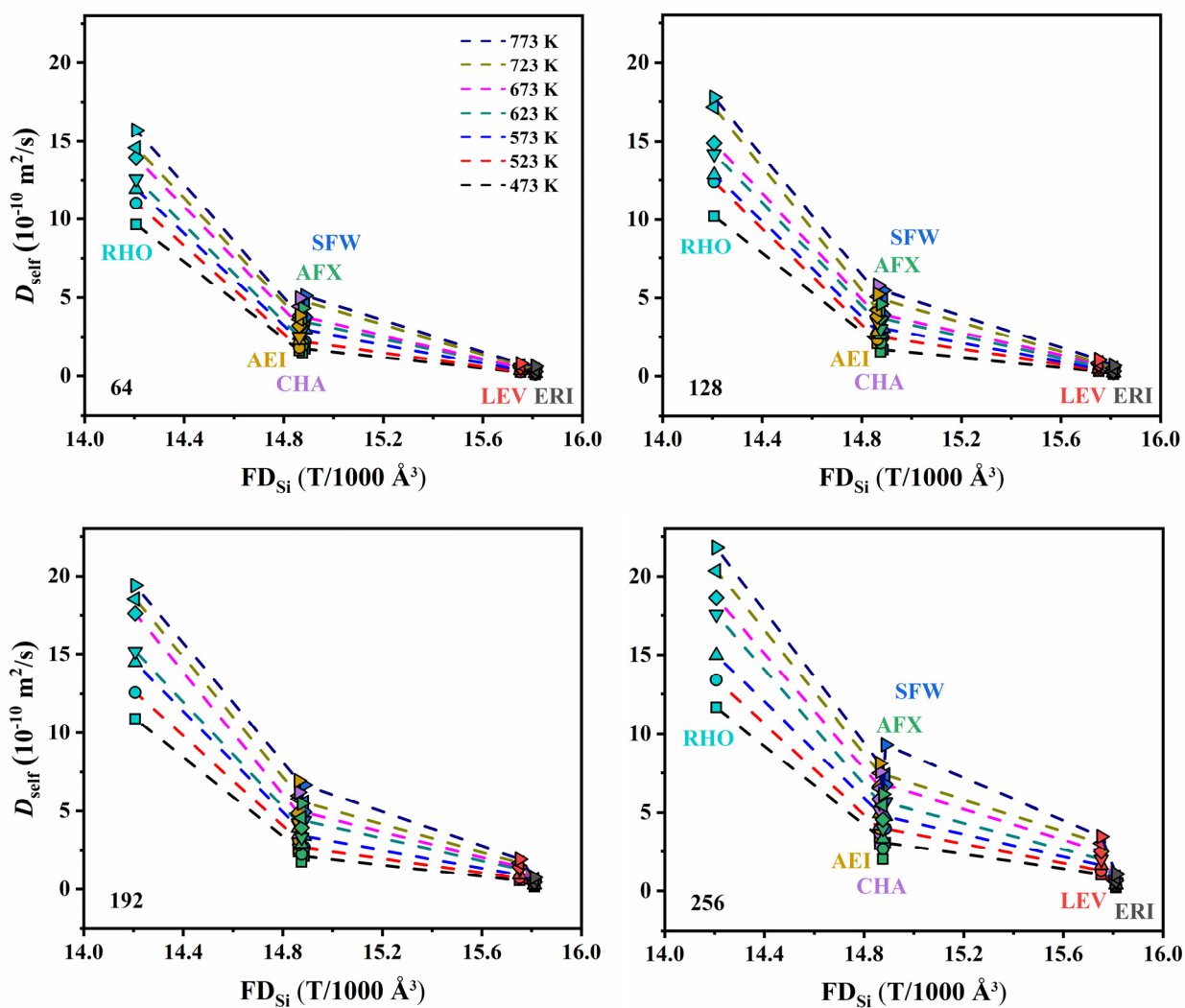


Fig. S8 Variation of the self-diffusion coefficient of ethene with the loading in seven zeolites at seven temperatures.



**Fig. S9** Variation of the self-diffusion coefficient of ethene with the pore diameter ( $d_m$ ) of the 8-ring in seven zeolites at seven temperatures and four loadings.



**Fig. S10** Variation of the self-diffusion coefficient of ethene with the framework density ( $\text{FD}_{\text{Si}}$ ) in seven zeolites at seven temperatures and four loadings.



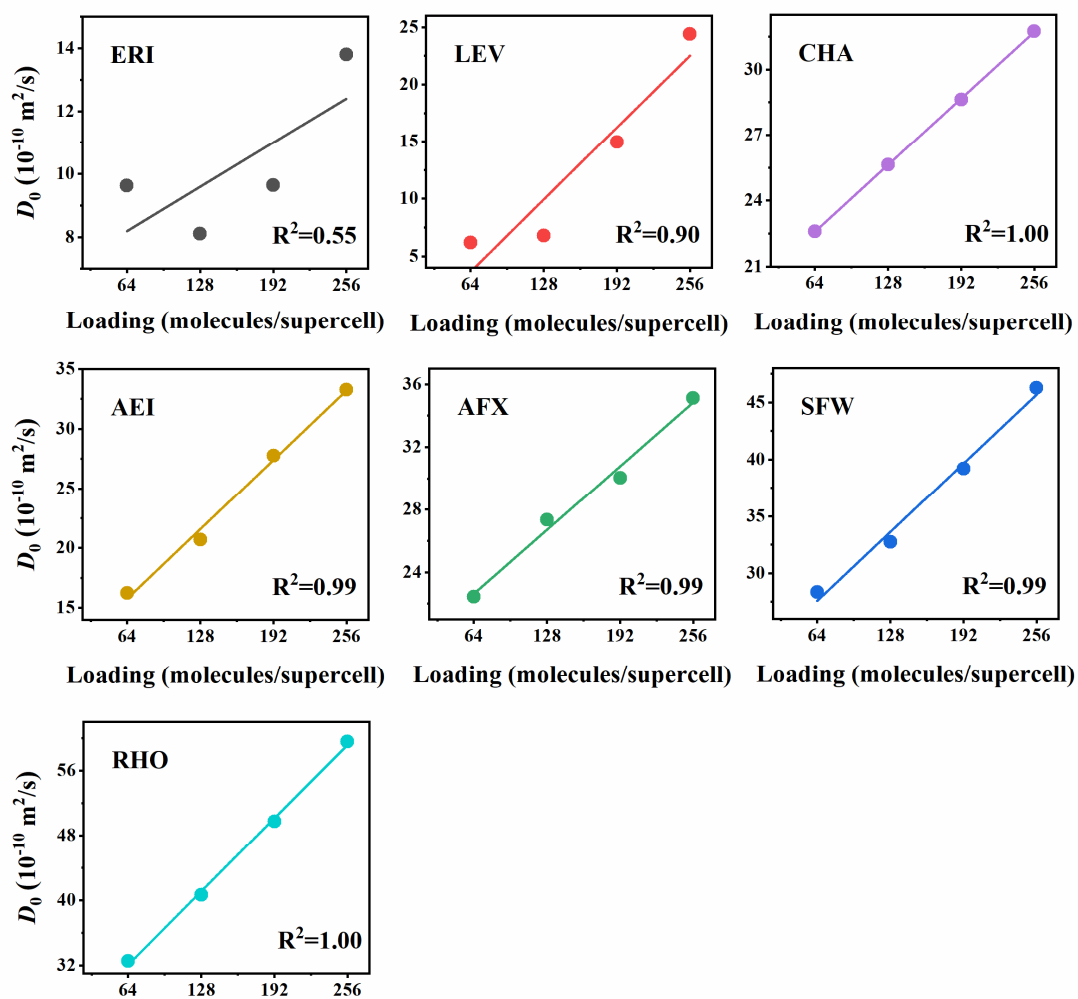
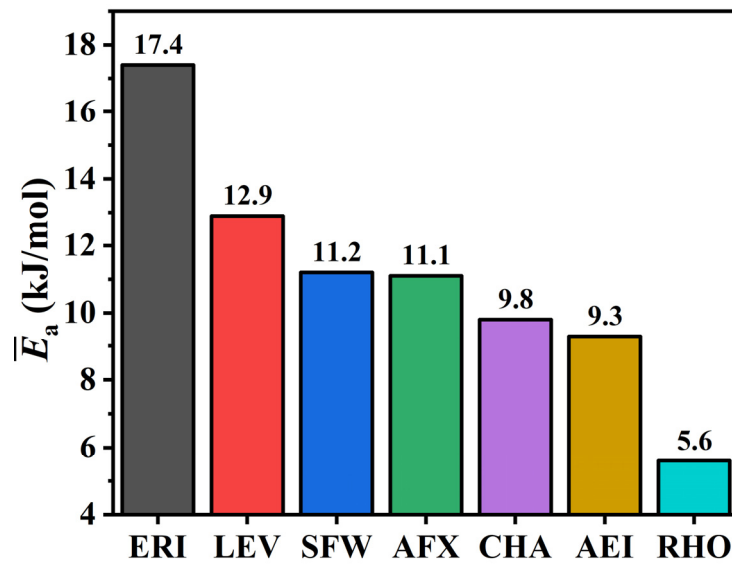
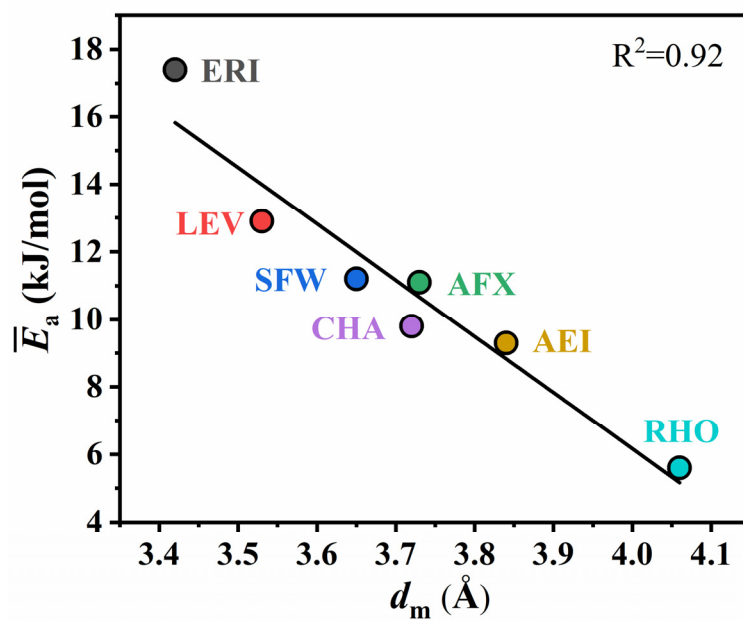


Fig. S11 Relations between the pre-exponential factor and the loading for ethene diffusion in seven different zeolites.



**Fig. S12** Histogram of the averaged activation energy of ethene diffusion in seven zeolites.



**Fig. S13** Scaling relation between the averaged activation energy and the maximum diameter of a sphere that can diffuse along 8-ring of zeolites taken from IZA ([https://asia.iza-structure.org/IZA-SC/ftc\\_table.php](https://asia.iza-structure.org/IZA-SC/ftc_table.php)) for the diffusion of ethene in seven zeolites.

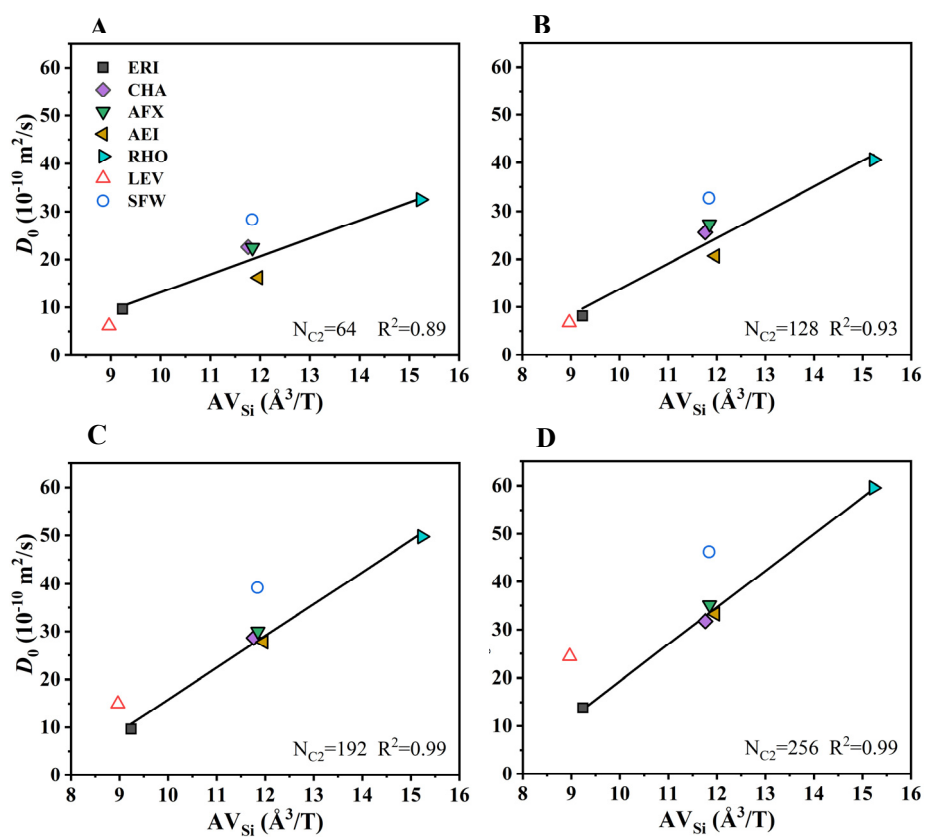


**Fig. S14** Scaling relations between the pre-exponential factor and the accessible volume of each Si atom in ERI, CHA, AFX, AEI, and RHO zeolites at different ethene loadings. The values in LEV and SFW are listed for comparison.